LONG-TERM TRENDS IN EXTREME PRECIPITATION INDICES OVER CACHAR DISTRICT OF ASSAM : 1901-2021

Abhay Bhattarai*[1] and Atri Deshamukhya[1]

[1]*Department of Physics, Assam University, Silchar 788011, Assam, India*

*Corresponding Author: abhaybhattarai@gmail.com

(Received 20 December 2025; revised 6 February 2025; accepted 21 February 2025; published 7 April 2025)

Abstract: This study investigates long-term trends in extreme precipitation indices over Cachar district, Assam, from 1901 to 2021, focusing on their spatial and temporal variations and implications for urban flood management. Using gridded rainfall data and indices defined by the Expert Team on Climate Change Detection and Indices (ETCCDI), the analysis reveals significant changes in precipitation patterns, including increases in very heavy rainfall (R50mm) during annual, monsoon, and pre-monsoon periods. Conversely, moderate (R10) and heavy (R20) rainfall frequencies show a declining trend, while daily precipitation intensity (SDII) has increased, particularly in pre-monsoon seasons. The study employs the Modified Mann–Kendall (MMK) test at a 95% confidence level and Sen's slope estimator for trend analysis, highlighting an increasing trend in extreme events like R1day and a significant reduction in consecutive wet days (CWD). These findings underscore the need for improved urban flood mitigation strategies, especially as intense precipitation events become more frequent in Cachar district. This work provides critical insights into the impact of climate variability on hydrological systems, emphasizing the role of sustainable urban planning in addressing future climate challenges.

Keywords: Extreme Precipitation Indices, Climate Variability, Urban Flooding, Modified Mann–Kendall Test.

PACS: 92.60.Jq, *92.60.jf, 92.40.Ea, 92.70.Mn

1 Introduction

The north-eastern part of India experiences significantly heavier rainfall compared to other regions of the subcontinent. This region faces two major challenges linked to climate change: high-intensity rainfall over short durations and prolonged dry spells. These challenges necessitate careful planning and management of water resources, with climate change being a crucial consideration. Several studies have focused on the impact of climate change on water resources across the northeastern region of India, primarily analyzing the precipitation and streamflow characteristics of the Brahmaputra River and its tributaries [1, 2, 3]. However, the Barak River, which flows parallel to the Brahmaputra in northeast India, exhibits a distinct climatic scenario. Receiving predominantly orographic and cyclonic precipitation, the Barak Basin averages 300 cm of rainfall annually and spans an area of 41,000 km², making it one of India's largest basins. Silchar, the most densely populated town in South Assam within the Barak Basin, is particularly vulnerable to heavy rain influxes during the monsoon and pre-monsoon seasons. The town's population has seen significant growth—from 34,000 in 1951 to 1.72 lakhs in 2011—along with unsystematic urban expansion. Poor urban planning, lack of proper drainage systems, and unregulated construction activities have compounded the town's vulnerability to flooding. Many areas previously unaffected by waterlogging are now inundated annually, creating severe challenges for local authorities.

Climate change, characterized by long-term climate variability over decades or more, impacts both global and regional precipitation patterns. Studies show that annual precipitation has increased by 1.5% over the past decade in the northern hemisphere [4]. Furthermore, average precipitation has increased by 7-12% in the zones 30°N-85°N and by 2% in the zones 0°S-55°S over the last century [5]. For a country like India, where rainfall significantly influences economic performance and social progress, understanding climate variability is paramount.

While much of the observed meteorological variability can be attributed to anthropogenic activities, it remains difficult to detect changes due to their gradual nature. Climatic trends are also influenced by factors such as dataset time spans, variability, and external events like volcanic eruptions or regional climatic changes [6, 7]. In India, studies over the last four decades have generally found monsoon rainfall to be trendless and random on a national scale [8, 9, 10]. However, localized areas, such as the Barak Basin, exhibit significant long-term changes in rainfall patterns [11].

Rapid urbanization, population growth, poor urban planning, and extreme climate events have led to artificial flooding in urban regions like Silchar. This highlights the importance of monitoring extreme weather events, especially during pre-monsoon and monsoon seasons, to better address flood-related challenges. To understand these changes, the Expert Team on Climate Change Detection and Indices (ETCCDI) developed 27 indices to analyze extreme weather events using daily temperature and precipitation data [12]. Despite some literature on rainfall trends in the Barak Basin, studies involving satellite-based data or detailed analyses of extreme precipitation indices in this region remain scarce [13].

Numerous non-parametric methods have been employed in previous studies to detect trends and variations in hydrological and climatic variables across Northeast India [11, 12, 13, 14, 15, 16]. Unlike parametric methods, which assume an underlying normal distribution and require both distributional and independence assumptions to be met, non-parametric methods do not rely on fixed parameters or a specific distribution and only require the data to be independent [17]. This flexibility makes non-parametric approaches particularly suitable for analyzing trends in climatic variables such as rainfall, temperature, and other environmental parameters. The Mann-Kendall (MK) test has become one of the most widely used methods for trend analysis in recent years because it does not require data to follow a normal distribution and is relatively insensitive to sudden changes caused by inhomogeneities in time series data [15, 16, 17]. However, trend tests require data to be independent, but the presence of positive serial autocorrelation can increase the likelihood of detecting significant trends. To address this, researchers recommend either removing serial correlation before applying trend tests or modifying existing methods to account for it [18]. To mitigate the impact of serial correlation, Hamed and Rao (2008) introduced the Modified Mann-Kendall (MMK) test [18], which adjusts for autocorrelation effects [19]. Given its advantages, MMK has been utilized in this study. Additionally, previous research by Bora et al. (2022) [15] demonstrated that the MMK test was more effective in detecting significant changes in rainfall trends compared to other similar methods such as Mann-Kendall, trend-free pre-whitening Mann-Kendall and innovative trend analysis (ITA).

This study focuses on analyzing rainfall trends and extreme precipitation events during the pre-monsoon and monsoon seasons in Cachar district, Assam. Using 10 extreme precipitation indices, spatial and temporal variations of rainfall will be studied. Trends in meteorological variables will be evaluated using the Modified Mann Kendall (MMK) test and Sen's slope estimator. Insights gained from this study will contribute to urban flood management and sustainable planning for mitigating climate-induced risks in the region.

2 Data and Methodology

The study is carried out over a small region (24.25°-25.25° N; 92.5°-93.5° E), area under the Barak Valley of Assam during 1901-2021 over the different season. The study region is shown in figure 1. The study area comprises of 25 grids and we have selected all the 25 grids for the study and for the study of Cachar district a total of 8 grids are selected. Our focus of the study is over the urban area of the Cachar district. As Silchar town is the prime urbanised area in the district and often indulged due to the continuous urban flooding in the area during the pre-monsoon and monsoon season. In recent period the Silchar town and municipal area surrounding it, experienced heavy flood for many days during the pre-monsoon and in the monsoon season.

2.1 Rainfall Data

For the long-term trend of the rainfall over the Cachar region, the high resolution gridded (0.25×0.25) daily rainfall data is utilised for a period of 1901-2021. The dataset, developed by the India Meteorological Department (IMD), incorporates data from approximately 6,955 operational rain gauge stations across India. To ensure reliability, the dataset underwent extensive quality control, addressing issues such as missing data and correcting anomalies or outliers in recorded rainfall values [20].

2.2 Extreme precipitation indices

This study uses a set of rainfall indices developed by the Expert Team on Climate Change Detection and Indices (ETCCDI) to understand extreme weather events [12]. These indices are based on daily rainfall data and help analyze how much it rains, how intense the rain is, and how often extreme rain happens. We chose 10 indices for this study (see table 1). These indices can be grouped into two categories:

1. **Amount and intensity**: These measure how much rain falls (like the heaviest one-day or five-day rainfall) and how intense the rain is on average each day.

2. **Frequency and duration**: These track how often moderate, heavy, or very heavy rainfall occurs and how long dry or wet spells last.

Using these indices, we can better understand patterns like heavy rainfall that might cause floods or long dry spells that could affect farming and water availability. This information helps us study rainfall changes in a clear and detailed way.

2.3 Trend analysis

The traditional quality Control methods assume normality for simplicity, standardization, and statistical convenience, but real-world time series data often deviate from this assumption, necessitating non-parametric or distribution-free methods for robust quality control. Especially in climate, hydrology, finance, and environmental studies, where data may be skewed, heavy-tailed, or contain seasonal trends. This is why non-parametric tests (like the Mann-Kendall (MK), Modified Mann-Kendall (MMK), Pettitt's Test) are preferred for trend detection in such cases. To study rainfall patterns over time, this research uses the Modified Mann-Kendall (MMK) test, a widely used method for analyzing trends in environmental data like rainfall and temperature. The MMK test is a non-parametric method, meaning it does not assume that the data follows a specific pattern, such as a normal distribution [19]. This makes it suitable for datasets with irregularities, such as missing values or outliers, which are common in long-term climate data. To explain the detailed methodology of the MMK we need to look into the predecessor Mann Kendall test.

2.3.1 Mann-Kendall test

The Mann-Kendall (MK) test is a widely used non-parametric statistical test for detecting trends in hydrometeorological and climate-related time series data [21, 22]. The fundamental objective of the MK test is to determine whether a **monotonic trend** (either increasing or decreasing) exists within a dataset over time, without making assumptions about its linearity. This is achieved by examining the relative ordering of values within the time series rather than their absolute magnitudes. The MK test is based on the Mann-Kendall statistic (S), which evaluates the number of increasing and decreasing values in the dataset. If the number of increasing values significantly exceeds the number of decreasing values, it suggests an upward (positive) trend in the variable under study. Conversely, a larger number of decreasing values indicates a downward (negative) trend. When the increasing and decreasing values are roughly equal, no significant trend is detected.

The presence of statistically significant trend of statistic S is checked using the standardized test statistic (Z). The MK test checks for the null hypothesis of no trend versus the alternative hypothesis of the existence of increasing or decreasing trend [13, 14, 15]. The MK statistic (S) is defined as.

$$S = \sum_{k=1}^{n-1} \sum_{j=k+1}^{n} \operatorname{sign}(x_j - x_k) \tag{1}$$

Where n is the number of data points. x_j and x_k are the observed value at time j and k such that $j > k$. The value of $\operatorname{sign}(x_j - x_k)$ is calculated as

$$\operatorname{sign}(x_j - x_k) = \begin{cases} 1 & \text{if } (x_j - x_k) > 0 \\ 0 & \text{if } (x_j - x_k) = 0 \\ -1 & \text{if } (x_j - x_k) < 0 \end{cases} \tag{2}$$

The variance $\mathrm{Var}(S)$ is defined as

$$\mathrm{Var}(S) = \frac{n(n-1)(2n+5) - \sum_{q=1}^{p} t_q(t_q-1)(2t_q+5)}{18} \tag{3}$$

Here p is the number of tied groups and t_q is the number of data point in the qth group. And the standard normal deviate (Z-statistics) is then computed as

$$Z = \begin{cases} \frac{S-1}{\sqrt{\mathrm{Var}(S)}} & \text{if } S > 0 \\ 0 & \text{if } S = 0 \\ \frac{S+1}{\sqrt{\mathrm{Var}(S)}} & \text{if } S < 0 \end{cases} \tag{4}$$

If the calculated value of $|Z| > Z_{\frac{\alpha}{2}}$, the null hypothesis H_0 is rejected at level of significance in a two-sided test, where depicts significance level 0.05 (e.g. 5% with $Z_{0.0025}$ =1.96). the null hypothesis is tested at a confidence level of 95%.

2.3.2 Modified Mann Kendall test

It is always preferable to do the autocorrelation or serial correlation while doing the time series analysis. Autocorrelation increases the chance of detection of the any kind of trend decreasing or increasing. So, as proposed by Hamed and Rao [18, 19] the corrected variance for the Modified Mann Kendall test is

$$\mathrm{Var}(S)^* = \mathrm{Var}(S) \times \mathrm{CF} \tag{5}$$

where CF is the correction factor given by

$$\mathrm{CF} = 1 + \frac{2}{n(n-1)(n-2)} \sum_{i=1}^{p} (n-i)(n-i-1)(n-i-2)p_s(i).$$

This leads to

$$\mathrm{Var}(S)^* = \frac{1}{18}\left[n(n-1)(2n+5)\right]\left[1 + \frac{2}{n(n-1)(n-2)} \sum_{i=1}^{p} (n-i)(n-i-1)(n-i-2)p_s(i)\right]. \tag{6}$$

In this equation, n is the number of observations in the sample, $p_s(i)$ is the autocorrelation between the ranks of the observation for lag i and p is the maximum time lag under consideration.

The Modified Mann-Kendall (MMK) test is an adaptation of the traditional Mann-Kendall (MK) test, designed to account for the influence of serial autocorrelation in time series data. The classic Mann-Kendall test assumes that the observations are independent of one another, which is a common assumption in statistical trend analysis. However, in real-world data, especially in fields like hydrology, climatology, and environmental sciences, time series often exhibit autocorrelation, meaning that consecutive data points are not independent, but instead are related to each other. In situations where positive serial autocorrelation is present, the standard MK test may lead to incorrect conclusions by increasing the likelihood of detecting a false trend. This occurs because autocorrelation artificially inflates the statistical significance of trends. To address this issue, the MMK test incorporates a correction factor that adjusts for the effects of autocorrelation, thereby improving the reliability of trend detection in time series data.

Along with the MMK test, this study uses Sen's slope estimator to measure the magnitude of the trend. Sen's method calculates the median slope between all pairs of data points, providing a simple and robust way to determine how quickly the rainfall is increasing or decreasing. This approach is especially useful for detecting trends in hydrological and meteorological data, as it reduces the influence of extreme values or outliers.

2.3.3 Sen Slope estimator

Sen's method is widely used in determining the magnitude of the trend in the hydro-meteorological time series [23].

$$T_i = \frac{x_j - x_k}{j-k} \qquad for \;\; i = 1, 2, 3 \ldots\ldots. N \tag{7}$$

Where x_j and x_k are the data value at time j and k respectively and $j > k$. The median of the gives us the, Sen's Slope Estimator. The positive value of Q_i indicate the upward trend and the negative value indicates the downward trend in the time series.

$$Q_i = \begin{cases} T_{\frac{N+1}{2}}, & N \text{ is odd} \\ \frac{1}{2}\left(T_{\frac{N}{2}} + T_{\frac{N+2}{2}}\right), & N \text{ is even} \end{cases} \tag{8}$$

The combined use of the MMK test and Sen's slope estimator provides a clear and reliable understanding of how rainfall patterns have changed over the study period. Along with it the study adopts a clear approach for determining significant and non-significant trends. Unlike some previous studies [15, 16] that have employed varying alpha values or different confidence intervals for hypothesis testing of trend significance, this study maintains a consistent confidence level of 95% throughout [13, 19]. As we have used multiple Indices in our study the use of a fixed confidence interval is straightforward and consistent, making it easier to interpret results across different datasets and applications.

Indices	Name	Definition	units
R99p	Extremely wet days	Annual total precipitation when RR>99th percentile	mm
R95p	Very wet days	Annual total precipitation when RR>95th percentile	mm
R1day	Maximum 1-day precipitation amount	Monthly maximum 1-day precipitation	mm
R5day	Maximum 5-day precipitation amount	Monthly maximum consecutive 5-day precipitation	mm
SDII	Simple daily intensity index	Annual total precipitation divided by the number of wet days (defined as precipitation ≥1) in the year	mm/day
CWD	Consecutive wet days	Maximum number of consecutive days with RR<1 mm	day
CDD	Consecutive dry days	Maximum number of consecutive days with RR≥1 mm	day
R10	Number of moderate precipitation days	Annual count of days when RR ≥ 10 mm	day
R20	Number of heavy precipitations days	Annual count of days when RR ≥ 20 mm	day
R50	Number of very heavy precipitation days	Annual count of days when RR ≥ 50 mm	day

Table 1: Extreme precipitation indices

3 Results and Discussion

3.1 Statistics of the rainfall

The monthly, seasonal and annual mean, standard deviation and coefficient of variation of the 121 years of rainfall over the overall study region is given in table 2.

MONTHS	MEAN (MM)	SD	COV (%)
JAN	13.83	17.95918	129.8567
FEB	38.07	36.67468	96.33485
MAR	101.93	77.72074	76.24914
APR	211.79	116.5278	55.02046
MAY	282.45	117.2772	41.5214
JUN	416.88	120.8245	28.98304
JUL	403.53	86.41284	21.41423
AUG	368.46	90.63331	24.59787
SEP	276.28	84.34041	30.52715
OCT	149.76	73.09617	48.80887
NOV	37.2	47.50578	127.7037
DEC	11.14	19.05873	171.0838
MONSOON	1465.14	217.4528	14.84178
POSTMONSOON	186.96	84.2729	45.07536
PREMONSOON	596.18	176.6677	29.63327
ANNUAL	2311.31	337.3837	14.59707

Table 2: Basic statistical characteristics of the 121 years precipitation over the study region

During the monsoon season, June stands out as the wettest month, with an average monthly rainfall of 416.88 mm, followed closely by July at 403.53 mm and August at 368.46 mm. These months collectively contribute significantly to the region's annual precipitation, reflecting the monsoon's intensity during this period. December receives the least rainfall, marking a sharp decline as the region transitions into the drier winter months. Additionally, figure 1 illustrates the spatial distribution of annual and seasonal mean rainfall, as derived from IMD-gridded data, for the period 1901-2021. The figures clearly demonstrate that the monsoon season significantly contributes to the total annual rainfall, with the pre-monsoon season providing a notable secondary contribution.

A distinct spatial pattern is evident, with precipitation levels declining from the northwest towards the southern parts of the region during the annual period. During the monsoon season, this decline follows a slightly different trajectory, decreasing from west to east. A similar trend of diminishing rainfall is observed across other seasons, underscoring the regional variability in precipitation patterns over the study area. These findings highlight the strong influence of both seasonal and spatial factors on rainfall distribution in the region.

The annual mean rainfall across the study area ranges from 1,477 mm to 3,110 mm per year, reflecting significant spatial variability. Within the Cachar district, the northwest region records the highest rainfall, reaching up to 3,310 mm annually, while the northeast experiences the lowest, at 1,803.6 mm per year. During the monsoon season, rainfall patterns follow a similar trend, with the northwest receiving a maximum of 1,948 mm per year and the northeast recording a minimum of 1,119.2 mm. The pre-monsoon season also makes a substantial contribution to the district's total annual rainfall, with values ranging from a high of 886 mm to a low of 437 mm annually. These variations underline the distinct seasonal and regional rainfall dynamics within the Cachar district.

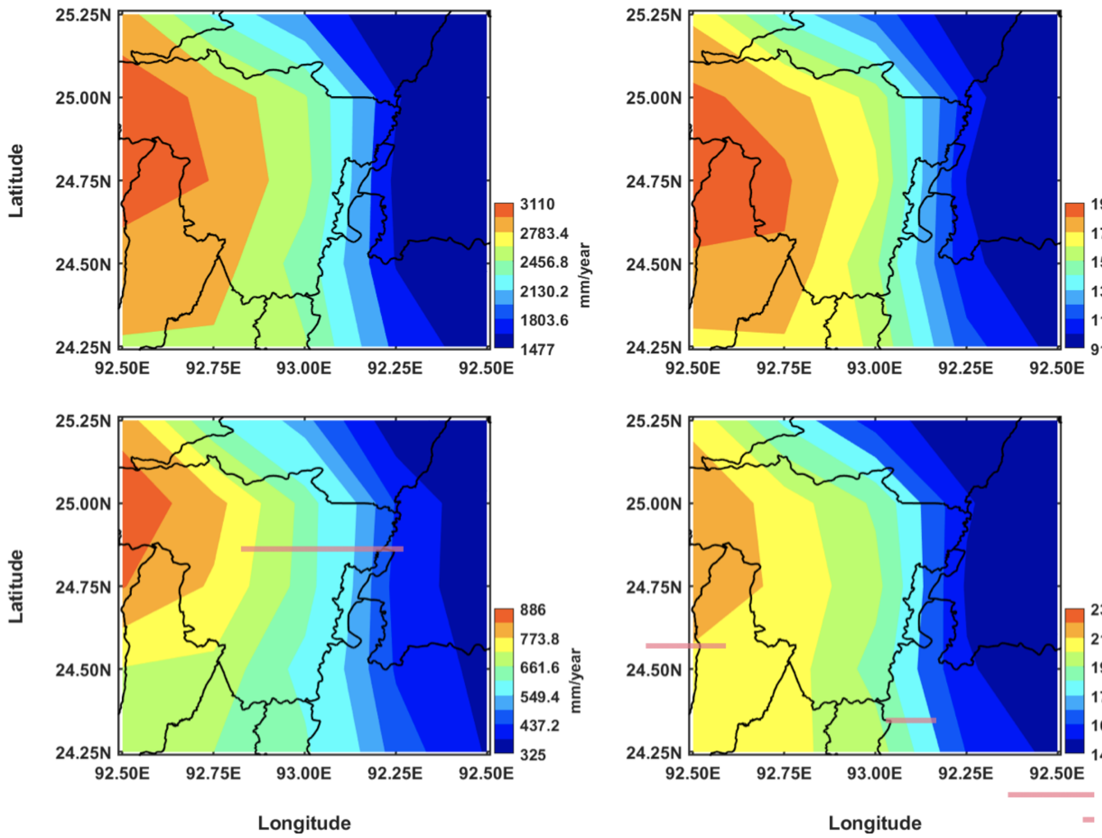

Figure 1: Spatial distribution of mean (a) annual, (b) monsoon, (c) pre-monsoon and (d) post-monsoon precipitation over a long term (1901-2021) in the study region.

3.2 Monthly and seasonal analysis

The non-parametric Modified Mann-Kendall (MMK) test, combined with Sen's slope estimator, was applied to analyze monthly and seasonal precipitation trends across the 121-year time series. The results, summarized in table 3, highlight monthly precipitation trends in terms of z values, slopes, and hypothesis testing. While considerable fluctuations were observed across months, significant trends were mostly absent, except for August. August exhibited the steepest declining trend, with rainfall decreasing at a rate of -0.77 mm/year, while January showed the smallest decline at -0.01 mm/year. In contrast, May demonstrated a slight increasing trend, with a growth rate of 0.34 mm/year. The significant decline in August underscores the variability in monthly rainfall patterns. For annual and seasonal precipitation, the analysis (as depicted in table 3 and figure 2) revealed an overall decreasing trend. The monsoon season exhibited a notable negative trend, with a z statistic value of -3.41 and a Sen's slope of -1.87 mm/year. Similarly, the annual trend showed a decline, with a z statistic value of -2.62 and a Sen's slope of -2.10 mm/year. These findings indicate a consistent reduction in both annual and seasonal rainfall during the study period (1901-2021).

The significant decline in monsoon rainfall has major implications for agriculture, water resources, and the economy of the region, as monsoon rains are the main source of annual precipitation. This decline drives the overall decrease in rainfall in the Cachar district, consistent with findings by [13] in the Barak Basin. Addressing this trend is crucial for ensuring agricultural sustainability and water security.

MONTHS	Z VALUE	SENSLOPE(MM/YEAR)	HYPOTHESIS
JAN	-0.66	-0.01	0
FEB	-1.70	-0.11	0
MAR	-0.84	-0.13	0
APR	-1.82	-0.51	0
MAY	0.99	0.34	0
JUN	-1.65	-0.41	0
JUL	-1.69	-0.33	0
AUG	-4.83	-0.77	1
SEP	-1.29	-0.25	0
OCT	-0.32	-0.06	0
NOV	-0.59	-0.04	0
DEC	0.54	0.00	0
MONSOON	-3.41	-1.87	1
POSTMONSOON	-1.22	-0.24	0
PRE-MONSOON	-0.70	-0.23	0
ANNUAL	-2.62	-2.10	1

Table 3: MK-test statistic and Sen's slope values along with Hypothesis result for 121 years monthly and seasonal precipitation

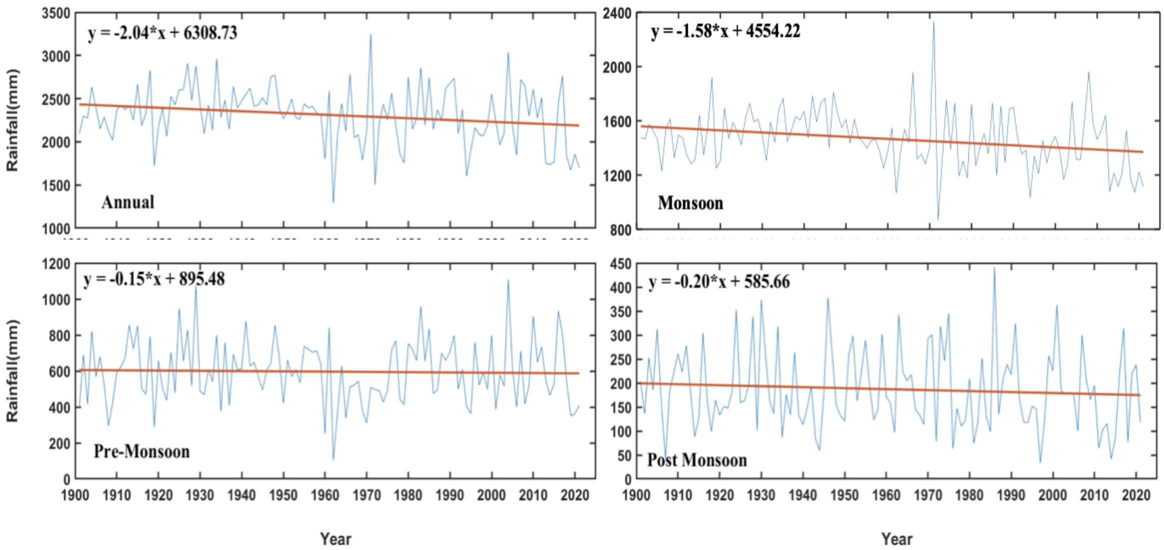

Figure 2: Temporal distribution of (a) annual (b) monsoon (c) pre-monsoon (d) post-monsoon precipitation of the region.

3.3 Annual characteristics of indices

The indices used to analyze extreme rainfall in the basin are detailed in table 1, and their trends, as well as changes in the frequency of heavy and very heavy rainfall days, are explained through extreme precipitation indices. Figure 3 illustrates the spatial distribution of these indices across the Cachar district for the period 1901-2021. Most magnitude and frequency indices, such as R99p, R95p, R1day, R5day, R10, R20, R50, and SDII, show an increasing trend from east to northwest, with the exception of consecutive dry days (CDD) and consecutive wet days (CWD), which follow a different spatial pattern. The annual precipitation corresponding to the 99th percentile ranges from 123 mm to 209 mm, increasing steadily towards the northwest. The western part of the study area, influenced by the hilly terrain of Meghalaya-one of the wettest regions globally-records the highest rainfall. A similar pattern is observed for R95p, with precipitation varying from 671 mm in the west to 403 mm in the east.

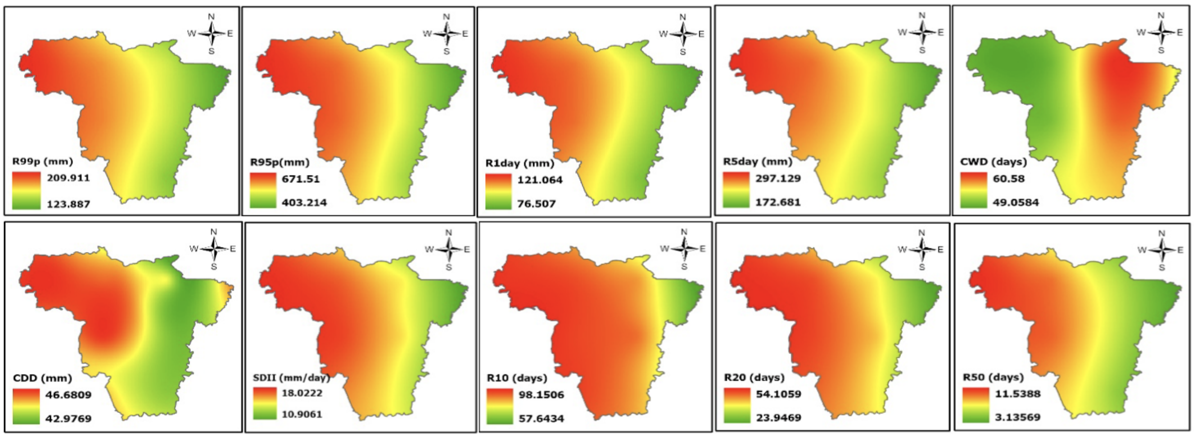

Figure 3: Spatial Distribution of mean annual extreme precipitation indices: R99p, R95p, R1day, R5day, CWD, CDD, SDII, R10, R20, R50 (left to right, top to bottom).

The R1day index, which represents the highest single-day rainfall in a year, is consistently high across the region, ranging from 76 mm to 121 mm, with higher values towards the northwest. Similarly, the R5day index, indicating the highest consecutive five-day rainfall, also follows this pattern, with values ranging from 171 mm to 297 mm. These observations underscore the pronounced spatial variability in extreme rainfall events within the Cachar district.

CDD (Consecutive Dry Days) and CWD (Consecutive Wet Days) are essential indicators for understanding the dry and wet conditions of a region, providing valuable insights for agricultural planning [12]. The highest CDD values are observed in the eastern part of the study area,reaching 42.9 days. Further northeast, the number of dry days slightly increases, peaking at 46.6 days in the northern and western directions. In contrast, CWD shows an average of 55 days, displaying an inverse spatial pattern to CDD. The lowest CWD values are concentrated in the north and northeast, while higher values are predominant in the northwestern part of the region.

The SDII (Simple Daily Intensity Index), which measures the intensity of daily rainfall, mirrors the spatial distribution of R99p and R95p. Most areas experience rainfall levels exceeding 18 mm, while the northeastern territory records lower intensity, around 10 mm. The frequency of days with daily rainfall exceeding 10 mm varies significantly, ranging from 99.15 days in the west to 59.64 days in the east, with notable contrasts in the northern areas. Similarly, the distribution of R20 (days with rainfall $\geq$ 20 mm) is aligned with R10 (days with rainfall $\geq$ 10 mm), although the frequency of R20 days is slightly lower in the eastern region. On the other hand, R50 (days with rainfall $\geq$ 50 mm) exhibits the highest values in the west at 11.53 days, gradually decreasing towards the east to a minimum of 3.13 days. The central part of the region displays average values within this range. These patterns highlight the spatial variability of rainfall intensity and frequency within the study area.

SEASONS	INDICES	SIGNIFICANT INCREASING TREND	SIGNIFICANT DECREASING TREND	NON-SIGNIFICANT INCREASING TREND	NON-SIGNIFICANT DECREASING TREND
ANNUAL	R99P	3	4	10	8
	R95P	7	6	4	8
	R1DAY	12	0	7	6
	R5DAY	5	4	9	7
	SDII	11	2	6	6
	CWD	0	22	1	2
	CDD	1	0	24	0
	R10	0	16	8	1
	R20	2	11	8	4
	R50	12	2	8	3
MONSOON	R99P	9	2	10	4
	R95P	4	6	9	6
	R1DAY	10	2	9	4
	R5DAY	1	5	10	9
	SDII	6	5	8	6
	CWD	0	22	0	3
	CDD	4	1	17	3
	R10	0	16	4	5
	R20	1	12	6	6
	R50	8	2	12	3
PRE-MONSOON	R99P	0	2	5	18
	R95P	3	4	10	8
	R1DAY	13	0	6	6
	R5DAY	6	1	11	7
	SDII	14	2	8	1
	CWD	0	21	1	3
	CDD	6	0	15	4
	R10	2	9	7	7
	R20	4	4	9	8
	R50	3	1	17	4
POST-MONSOON	R99P	0	0	0	0
	R95P	0	1	4	20
	R1DAY	0	1	14	10
	R5DAY	0	2	0	23
	SDII	5	0	8	3
	CWD	0	21	0	4
	CDD	2	0	23	0
	R10	0	9	5	11
	R20	0	2	7	16
	R50	0	0	13	11

Table 4: Significant and non-significant trends observed in the grids.

3.3.1 Spatial distribution of trend

The spatial distribution of the Significant and Non-significant trend of the extreme precipitation indices over the gridded region is given in table 4. It is clearly observed that most of the trend are non-significant, but a good amount of significant trend is also observed in region.

In the annual period more than 50% of the area shows an increasing trend for the extreme indices R99p, R5day and SDII, more than 70% is observed in R1day, 80% is observed in R50 and 100% is observed for the CDD. SDII and R1day observed a significant increasing trend in more than 40% of the region. R95p and CWD shows decreasing trend in 56% and 96% of the area respectively. It is interesting that CWD observed a significant decreasing trend in the 88% of the region. As R50 is showing a significant increase across more than 40% of the area and no-significant increase it also seen in other areas, gives an indication of the increase of the very heavy precipitation in area during the annual period.

In monsoon season it is clearly observed that the R95p, SDII, shows an increasing trend in more than 50% of the area. R99p, R1day observed increasing trend in more than 70% of the area. Where CDD and R50 shows a dominance over the 80% of the area with an increasing trend. It clearly indicates the increase of the very heavy precipitation and the increase of the consecutive dry days over the region. In this season a decreasing trend is observed for the CWD, R10, R20 in more than 70 percent of the region and R5day also observed decreasing trend for 56% of the area. This explains the decreasing of the moderate and heavy rainfall during the monsoon season in the region.

During the pre-monsoon season a decreasing trend is observed for the R99p, CWD, and R10 in more than 50% of the area. Whereas R95p, R1Day, R5day, SDII, CDD, R20, R50 observed increasing trend in more than 50% of the area. It is observed nearly 50% of the area shows a significant increasing trend for the single day maximum and SDII value. The increasing trend of the R50 explains the increasing of the very heavy rainfall during the pre-monsoon period over the study region. During the post monsoon period most of the results are insignificant. There is increasing trend of R50 in 52 % of the area and nearly all the region observes an increasing trend of CDD. A significant decrease of consecutive wet days is seen across more than 80% of the region.

4 Conclusions

The study highlights critical patterns of climate variability and changes in extreme precipitation, emphasizing the need for proactive management to address associated risks. Analysis of 10 widely recognized extreme precipitation indices reveals a significant increase in very heavy rainfall (R50 mm) during the annual, monsoon, and pre-monsoon seasons, while moderate (R10) and heavy rain (R20) exhibit consistent declining trends across much of the region. A marked decrease in consecutive wet days (CWD) is evident in nearly all parts of the region and across most seasons, while the Simple Daily Intensity Index (SDII) shows an increase in 60% of the area. This indicates a shift towards more intense rainfall during wet days, particularly during the pre-monsoon season, where increased rainfall intensity is linked to frequent flooding events. The R1day index also shows a significant upward trend in nearly half of the region, including the Cachar district, further underscoring the intensification of rainfall extremes.

Although consecutive dry days (CDD) are increasing, these trends are not statistically significant in most seasons. Overall, the findings indicate a decrease in wet indices paired with higher rainfall intensity per wet day, suggesting an escalation in very heavy precipitation events across the region, especially in the Cachar district. These insights underscore the urgent need to incorporate these trends into urban planning and flood mitigation strategies to better manage the impacts of increasingly extreme and variable rainfall. Proactive measures are essential to safeguard the region's agriculture, water resources, and urban resilience in the face of climate change.

5 Acknowledgements

The authors would like to thank the district authority of Cachar for providing support to carry out the study.

References

[1] A. K. Sarma, S. K. Deka, A study report, IIT Guwahati (2011).

[2] A. K. Sarma, P. K. Sarma, R. Vinnarasi, Report submitted to the Climate Change Directorate of MoWR, Govt. of India (2012).

[3] B. Kalita, A technical report, IIT Guwahati (2012).

[4] P. P. Mujumdar, D. N. Kumar, Cambridge University Press (2012).

[5] D. J. Griggs, M. Noguer, Weather 57, 267 (2002)

[6] S. Jain, U. Lall, Water Resour. Res. 36, 3641 (2000)

[7] E. C. Weatherhead, G. C. Reinsel, G. C. Tiao, X. L. Meng, D. Choi, W. K. Cheang, T. Keller, J. DeLuisi, D. J. Wuebbles, J. B. Kerr et al., J. Geophys. Res. Atmos. 103, 61 (1998)

[8] P. Guhathakurta, M. Rajeevan, D. Sikka, A. Tyagi, Int. J. Climatol. 35 (2014)

[9] S. D. Attri, A. Tyagi, Met. Monogr. No. Enviro Meteorology 1, 105 (2010)

[10] R. H. Kripalani, A. Kulkarni, S. S. Sabade, M. L. Khandekar, Nat. Haz. 29, 189 (2003)

[11] V. Kumar, S. K. Jain, Y. Singh, Hydrol. Sci. J. 55, 484 (2010)

[12] X. Zhang, L. Alexander, G. C. Hegerl, P. Jones, A. K. Tank, T. C. Peterson, B. Trewin, F. W. Zwiers, Wiley Interdiscip. Rev. Clim. Chang. 2, 851 (2011).

[13] S. Deb, B. S. Sil, Urban Clim. 30, 100530 (2019).

[14] N. Kamal, S. Pachauri, Int. J. Comput. Appl. 177, 7 (2019).

[15] S. L. Bora, K. Bhuyan, P. J. Hazarika, J. Gogoi, K. Goswami, Curr. Sci. 122, 801 (2022).

[16] V. Pandey, P. K. Pandey, B. Chakma, P. Ranjan, Environ. Sci. Pollut. Res. 31, 10359 (2024).

[17] P. Sonali, D. N. Kumar, J. Hydrol. 476, 212 (2013).

[18] K. H. Hamed, A. R. Rao, J. Hydrol. 204, 182 (1998).

[19] K. H. Hamed, J. Hydrol. 349, 350 (2008).

[20] D. S. Pai, L. Sridhar, M. Rajeevan, O. P. Sreejith, N. S. Satbhai, B. Mukhopadhyay, Mausam 65, 1 (2014).

[21] H. B. Mann, Econometrica 13, 245 (1945).

[22] M. G. Kendall, Griffin, 1948.

[23] P. K. Sen, J. Am. Stat. Assoc. 63, 1379 (1968).